JACS
JOURNAL OF THE AMERICAN CHEMICAL SOCIETY

COMMUNICATION

pubs.acs.org/JACS

Synthesis and Characterization of $Cu(In_xB_{1-x})Se_2$ Nanocrystals for Low-Cost Thin Film Photovoltaics

Lin-Jer Chen,[†] Jiunn-Der Liao,[*,†] Yu-Ju Chuang,[†] and Yaw-Shyan Fu[‡]

[†]Department of Materials Science and Engineering, National Cheng Kung University, Tainan, 701, Taiwan

[‡]Department of Greenergy Technology, National University of Tainan, 700, Taiwan

Supporting Information

ABSTRACT: Chalcopyrite quaternary semiconductor $Cu(In_xB_{1-x})Se_2$ nanocrystals have been successfully prepared via a relatively simple and convenient solvothermal route. The effect of different solvents on the formation of the product also indicates that diethylenetriamine is the optimal solvent for this reaction. The device parameters for a single junction $Cu(In_xB_{1-x})Se_2$ solar cell under AM1.5G are as follows: an open circuit voltage of 265 mV, a short-circuit current of 25.90 mA/cm^2, a fill factor of 34%, and a power conversion efficiency of 2.34%. Based on a series of comparative experiments under different reaction conditions, the probable formation mechanism of crystal $Cu(In_xB_{1-x})Se_2$ nanorods is proposed.

Multipart chalcogenide compound semiconductors have been regarded as one of the most promising materials for thin film solar cells because of their unique structural and electrical properties, high conversion efficiency, and low toxicity.[1−4] The chalcopyrite ternary semiconductor has been of interest as a crystalline thin film material for high efficiency solar cell applications.[5,6] However, the wide-spread utilization of I-III-VI_2 based solar cells has required the use of high-cost vacuum deposition techniques.[7,8] The creation of a suitable inorganic nanocrystal for use in a scalable wet-chemical process is a key step in the development of low-cost solar cells.[9−11] However, these methods require either very high temperature or special apparatus. In addition, these methods require a relatively long reaction time.

The device properties of I-III-VI_2 based solar cells are known to be critically influenced by their stoichiometric compositions, defect chemistry, and structure, which are strongly related to the preparation conditions. For example, the I-III-VI_2 film, which was made by controlling the size, shape, and composition of the layers at the nanoscale to form a reduced-dimensionality structure, has stronger absorption compared to bulk semiconductors.[12−18] Here, we present the first report of a new material, chalcopyrite $Cu(In_xB_{1-x})Se_2$ nanorods, and demonstrate that solvothermal based synthesis of these nanocrystals can be used to create simple solar cells, with our first cells exhibiting an efficiency of 2.34% under AM1.5 illumination. The main advantages of solvothermal synthesis are related to homogeneous nucleation processes due to elimination of the calcination step to produce very low grain sizes and high purity powders.[19−21] To the best of our knowledge, $Cu(In_xB_{1-x})Se_2$ has never been grown and studied. Boron should yield a higher band gap, closer to the ideal value of 1.5 eV, for lower concentrations of boron than either gallium or aluminum.[22] We have been interested in the use of a solvothermal route, which is carried out at low temperatures and does not require toxic precursors, to prepare $Cu(In_xB_{1-x})Se_2$ nanocrystals with a wide range of optical and electronic properties accessible in the nanoscale.

In our synthesis of the $Cu(In_xB_{1-x})Se_2$ nanocrystals, the order of addition of the boron precursor to a diethylenetriamine solution plays a major role in the resulting crystal structure of the final product. (Please see Supporting Information for experimental details.) As known, X-ray diffraction (XRD) is the most convenient and effective tool for investigation of a crystalline structure; however, the standard XRD patterns of $Cu(In_xB_{1-x})Se_2$ ($0 \le x \le 1$) could not be found in the literature and JCPDS card database. Nevertheless, we noticed that the XRD patterns of the chalcopyrite $Cu_xIn_ySe_{0.5x+1.5y}$ nanocrystals remain unchanged when the ratios of indium to gallium were 1:1.[23] Given their similar compositions, quaternary $Cu(In_xB_{1-x})Se_2$ nanocrystals should exhibit chalcopyrite crystalline structures similar to those of the $Cu_xIn_ySe_{0.5x+1.5y}$. XRD patterns of the samples prepared in diethylenetriamine are shown in Figure 1a. The average crystal domain size of the nanocrystals calculated using Scherrer's equation based on the (112) peak is 75 nm ($D = K\lambda/(\beta \cos \theta)$; $K = 0.89$, $\lambda = 0.15418$ nm, β = fwhm, θ = diffraction angle). The major diffraction peaks observed at 26.65°, 44.22°, 52.39°, 64.36°, 70.90°, and 81.38° 2θ can be indexed to the (112), (204)/(220), (116)/(312), (008)/(400), (316)/(332), and (228)/(424) of the sphalerite and chalcopyrite crystal structure, respectively. Thus, in order to determine that the nanocrystals are chalcopyrite, it is crucial to be able to observe the minor peaks that are unique to the chalcopyrite structure. For instance, the minor peaks at 17.14°, 27.74°, and 35.55° corresponding to the (101), (103), and (211) peaks, respectively, are unique to the chalcopyrite structure and are shown as an inset of Figure 1b. As the reaction time increases to 36 h, the three minor diffraction peaks could be obtained gradually, indicating that the sphalerite phase forms the chalcopyrite phase. According to the Vegard's law, the lattice constants measured for the $Cu(In_{0.9}B_{0.1})Se_2$ samples were $a = 5.556 \pm 0.003$ Å and $c = 11.151 \pm 0.003$ Å (as shown in Figure S1) with the $c/2a$ ratio of 1.003 ± 0.003. The observed lattice parameters and $c/2a$ ratio agree very well with the reported values for the chalcopyrite phase.[24] The

Received: October 15, 2010
Published: February 24, 2011

   dx.doi.org/10.1021/ja108812j | J. Am. Chem. Soc. 2011, 133, 3704–3707

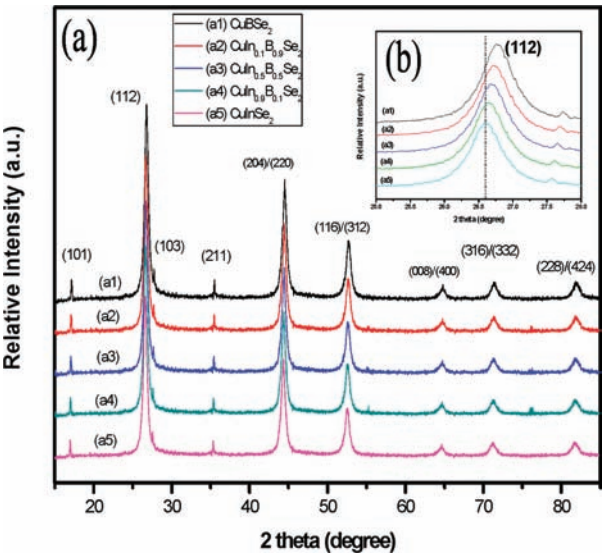

Figure 1. (a) XRD patterns of quaternary $Cu(In_xB_{1-x})Se_2$ nanocrystals synthesized by the solvothermal route for various indium/boron ratios. (b) The (112) patterns gradually shifting toward the higher diffraction angles with increasing boron content were obtained.

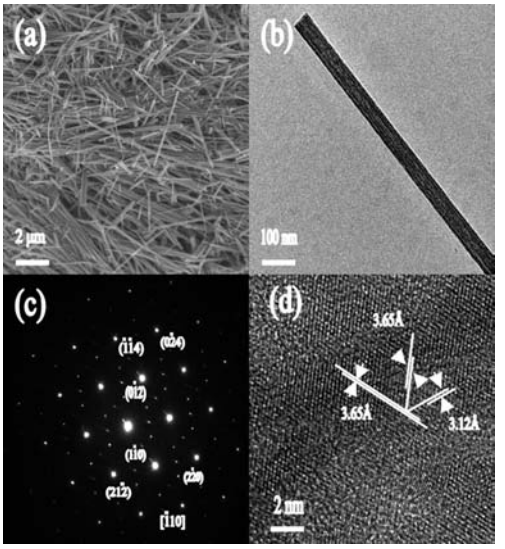

Figure 2. (a) SEM photoimage of the as-synthesized quaternary $Cu(In_{0.9}B_{0.1})Se_2$ nanorods. (b) TEM images of $Cu(In_{0.9}B_{0.1})Se_2$ nanorods. (c) SAED pattern of $Cu(In_{0.9}B_{0.1})Se_2$ nanorods. (d) High-resolution TEM of quaternary $Cu(In_xB_{1-x})Se_2$ nanocrystals recorded along $[\bar{1}10]$.

$Cu(In_xB_{1-x})Se_2$ nanocrystal diffraction peaks also show patterns gradually shifting toward a higher angle with increasing boron content, due to the decreased lattice spacing with smaller boron atoms substituting for larger indium atoms (Figure 1b). Similar behavior could be found in the literature.[25,26]

Figure 2 shows SEM and TEM images of chalcopyrite quaternary $Cu(In_xB_{1-x})Se_2$ nanocrystals prepared by solvothermal synthesis in diethylenetriamine at 180 °C for 36 h. The sample of $Cu(In_{0.9}B_{0.1})Se_2$ synthesized in diethylenetriamine appears to display a rod-like morphology with average widths of 70 ± 5 nm, which is in agreement with the XRD result of 75 nm calculated from the Scherrer formula. The image is taken along the $[\bar{1}10]$ zone axis with the $(2\bar{2}0)$, $(0\bar{1}2)$, and $(0\bar{2}4)$ crystallographic planes indicated by white lines. Spacing measurements based on 10 planes indicated *d*-spacings of 3.12 ± 0.02 Å for $(2\bar{2}0)$ and 3.65 ± 0.02 Å for $(0\bar{1}2)$ and $(0\bar{2}4)$. The measured angle between the $(2\bar{2}0)$ and $(0\bar{2}4)$ planes is 56.9 ± 0.2° and is 66.2 ± 0.2° between $(0\bar{1}2)$ and $(0\bar{2}4)$ planes. If the structure were sphalerite, the measured angles should be 60° between all three planes, and the measured *d*-spacings should be 3.47 Å. The zone axis of the selected-area electron diffraction (SAED) pattern was determined to be $[\bar{1}10]$, and the pattern is typical for nanocrystals from this same synthesis procedure. We also observed additional diffraction spots, circled in white in Figure 2c. These extra spots correspond to 2/3 the distance of the $(\bar{1}\bar{1}\,4)$ or $(21\bar{2})$ fundamental reflections and have a *d*-spacing of 3.6 Å in Figure 2d. Both high-resolution TEM (Figure 2d) and XRD (Figure 1a) confirmed that the nanocrystals are crystalline with a chalcopyrite ternary structure. Furthermore, an XPS survey with CasaXPS software calculation provided the quantitative information about chalcopyrite ternary film composition.[26−30] By taking the composition of the thin film as $Cu(In_xB_{1-x})Se_2$ and the element Se as the reference, the average composition of the nanocrystals in the sample remained as a relative atomic concentration of Cu/(In + B)/Se that was close to 1:1:2 with a variation from particle to particle of ca. ± 5.9 at% that is less than experimental error, as described in Figure S2. All four elements, i.e., copper, indium, boron, and selenium, were measured. To the best of the authors' knowledge, this is the first reported solvothermal synthesis of chalcopyrite quaternary $Cu(In_xB_{1-x})Se_2$ nanocrystals.

In this work, the solvent plays an important role in the formation of the chalcopyrite quaternary $Cu(In_xB_{1-x})Se_2$ nanocrystals. Diethylenetriamine was selected as the solvent due to its strong basic capacity and strong chelation.[31] It is well-known that boron oxide, indium chloride, and Se powders are soluble in diethylenetriamine at room temperature. In the solvothermal route, a nucleophilic attack by diethylenetriamine can activate boron oxide (or indium chloride) and elemental selenium to form B^{3-} (or In^{3+}) and Se^{2-} ions. Furthermore, in this electron transfer reaction, diethylenetriamine, as a reducing solvent, can reduce Cu^{2-} to Cu^{-} ion and then Cu^{-} complexes with diethylenetriamine to form $[Cu(DIEN)_2]^+$.

In addition, diethylenetriamine plays an important role in controlling the nucleation and growth of the product. Because of its N-chelation and special structure, it can easily chelate Cu^+ (reduced from Cu^{2+}) and form a relatively stable complex $[Cu(DIEN)_2]^+$. The formation of the complex can effectively prevent the formation of binary copper chalcogenides. To improve our understanding of the above mechanism, experiments were performed under similar conditions when diethylenetriamine was replaced by other solvents such as ethylenediamine and oleylamine. In oleylamine, many diffraction peaks appeared in the XRD patterns which could be indexed to copper selenide, and copper boron, but no characteristic peaks of chalcopyrite structure appeared. In ethylenediamine, a longer reaction time (at least 72 h) was required in order to obtain the product with almost the same morphology as that in diethylenetriamine. The above results indicate that diethylenetriamine is the optimal solvent for this reaction. In our work, the growth habits always directly determine the final crystal shape, which in turn is greatly influenced by its growth conditions. On the basis of the evolution of time-dependent morphologies, as shown in Figure S3, we hypothesize that the formation of nanostructures and morphologies developing from particles to rods can be

dx.doi.org/10.1021/ja108812j |*J. Am. Chem. Soc.* 2011, 133, 3704–3707

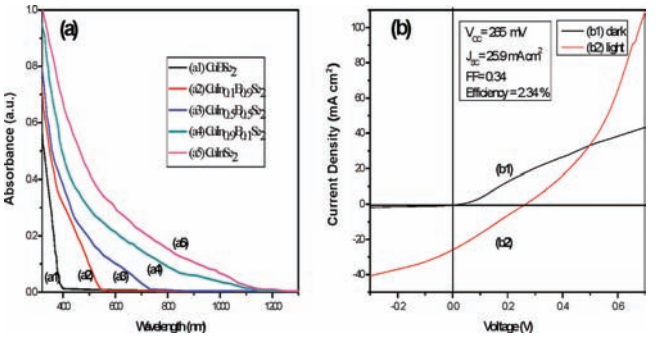

Figure 3. (a) UV/vis absorption spectra of $Cu(In_xB_{1-x})Se_2$ nanocrystals dispersed in toluene. The curves correspond to [B]/[In] + [B] stoichiometries of x = (a1) 1, (a2) 0.9, (a3) 0.5, (a4) 0.1, and (a5) 0. (b) Current−voltage characteristics by the AM1.5 irradiation (100 mW/cm^2). The nanocrystal absorber layer was 800 nm thick, consisting of diethylenetriamine capped $Cu(In_{0.9}B_{0.1})Se_2$ nanocrystals with an average diameter of 75 nm.

rationally expressed as a nucleation−dissolution−recrystallization mechanism.[32,33] The $Cu(In_xB_{1-x})Se_2$ nanocrystals with irregular shapes were formed in the solution through a homogeneous nucleation process. During the solvothermal route, a large quantity of $Cu(In_xB_{1-x})Se_2$ nuclei were first formed due to the decomposition of a part of B_2Se_3, In_2Se_3, and CuSe precipitates. On the other hand, certain B_2Se_3, In_2Se_3, and CuSe precipitates transformed into the growth units of $(BSe_2)^-$, $(InSe_2)^-$, and $[Cu(DIEN)_2]^+$ under alkaline conditions. As a consequence, the rod-like $Cu(In_xB_{1-x})Se_2$ crystals were formed.

Figure 3 a shows UV/vis absorption spectra and optical micrographs of the chalcopyrite quaternary $Cu(In_xB_{1-x})Se_2$ nanocrystals synthesized by a solvothermal route at 180 °C for 36 h. Consistently, the band gap absorption of the $Cu(In_xB_{1-x})Se_2$ nanocrystals gradually red shifts with decreasing boron composition. According to the band-structure theory,[22] the optical band gaps of the $CuBSe_2$ and $CuInSe_2$ nanocrystals are around 3.13 and 1.05 eV, respectively, which are close to those of the bulk $CuBSe_2$ (3.17 eV) and $CuInSe_2$ (1.04 eV).[22,34] Boron should yield a higher energy band gap, closer to the ideal value of 1.5 eV, for lower concentrations of boron than either gallium or aluminum. Consistent with the color change, the band gaps of $Cu(In_xB_{1-x})Se_2$ nanocrystals can be readily tuned between 3.13 and 1.05 eV by adjusting the ratios of boron (i.e., relatively small in size and dimension) to indium. Theoretical calculation shows that the band gap of this new material $CuBSe_2$ (CBS) should be 3.17 eV. To estimate this value, the band gaps of $Cu(In_xB_{1-x})Se_2$ were fitted by an exponential function using the following band-structure theory eq 1:[22]

$$E_{g(CuIn1-xYxSe2)} = (1-x)E_{g(CuInSe2)} + xE_{g(CuYSe2)} - bx(1-x) \quad (1)$$

where E_g is a band gap, Y represents an element of the group IIIA in the periodic table, x is the fraction of Y concentration, and b is a parameter, which ranges from −0.07 to 0.28.

In this work, the first batch of thin film solar cells was fabricated by drop-casting the $Cu(In_xB_{1-x})Se_2$ absorber layer, followed by chemical bath deposition of a CdS layer, RF sputtering of 60-nm intrinsic zinc oxide, and then 200 nm of ITO layers (see experimental details in the Supporting Information). The corresponding $I-V$ characteristic of the solar cell is shown in Figure 3 b. The final devices are scribed into small areas of 0.124 cm^2 with a small dap of silver paint applied to form the top contact. The device parameters for a single junction $Cu(In_xB_{1-x})Se_2$ thin film solar cell under AM1.5G are as follows: an open-circuit voltage of 265 mV, a short-circuit current of 25.90 mA/cm^2, fill factor of 34%, and a power conversion efficiency of 2.34%. Device efficiencies might be improved by increasing the $Cu(In_xB_{1-x})Se_2$ film thickness to absorb more photons. However, a lower fill factor due to high series resistance causes lower performance of the present device. Overall, the fill factor of the $Cu(In_xB_{1-x})Se_2$ devices are lower than those typically reported for high-efficiency CIGSe solar cells, partly due to the large amount of dark areas from the silver contacts and shadow from the probe.

In summary, we have successfully synthesized multiple component chalcopyrite semiconductor $Cu(In_xB_{1-x})Se_2$ nanocrystals via a relatively mild and convenient solvothermal route. The solvent plays an important role in the formation of the product, and diethylenetriamine is the optimal solvent for this reaction. The size of the resulting nanorods could be controlled under a temperature of 180 °C for 36 h. The $Cu(In_xB_{1-x})Se_2$ nanocrystals with an average diameter of 75 nm were obtained. However, we believe that the synthesis process played a very important role in the result, because only the solvothermal route with diethylenetriamine as a solvent was found to be effective to form crystalline nanorods. Equivalent boron was introduced into the $Cu_xIn_ySe_{0.5x+1.5y}$ nanocrystals to partly replace the indium, forming multipart nanocrystals with broad compositional ranges. The optical band gap and lattice parameters of the alloyed nanocrystals are composition- dependent, following the equation and Vegard's law. These nanocrystals have good solubility in organic solvents (toluene, hexane, and amine solvent) and may be potentially used as absorber and window materials in multijunction photovoltaic cells and other applications.

■ ASSOCIATED CONTENT

Supporting Information. Detailed information on nanocrystal preparation and characterization, device fabrication, the lattice constants, and SEM images of CIBS morphology. This material is available free of charge via the Internet at http://pubs.acs.org.

■ AUTHOR INFORMATION

Corresponding Author
jdliao@mail.ncku.edu.tw

■ ACKNOWLEDGMENT

The study was supported by Top 100 University Advancement and the collaboration of Center for Micro/Nano Science and Technology of National Cheng Kung University, under Grant Nos. D99-2700 and D99-3300.

■ REFERENCES

(1) Slaoui, A.; Collins, R. T. *Mater. Res. Bull.* **2007**, *32*, 211.
(2) Paulson, P. D.; Haimbodi, M. W.; Marsillac, S.; Birkmire, R. W.; Shafarmana, W. N. *J. Appl. Phys.* **2002**, *91*, 10153.
(3) Repins, I.; Contreras, M. A.; Egaas, B.; DeHart, C.; Scharf, J.; Perkins, C. L.; To, B.; Noufi, R. *Prog. Photovoltaics* **2008**, *16*, 235.
(4) Marsillac, S.; Paulson, P. D.; Haimbodi, M. W.; Birkmire, R. W.; Shafarman, W. N. *Appl. Phys. Lett.* **2002**, *81*, 1350.

(5) Gur, I.; Fromer, N. A.; Geier, M. L.; Alivisatos, A. P. *Science* **2005**, *310* (5747), 462.
(6) Joo, J.; Na, H. B.; Yu, T.; Yu, J. H.; Kim, Y. W.; Wu, F. X.; Zhang, J. Z.; Hyeon, T. *J. Am. Chem. Soc.* **2003**, *125* (36), 11100.
(7) Malar, P.; Das, V. D.; Kasiviswanathan, S. *Vacuum* **2004**, *75*, 39.
(8) Adurodija, F. O.; Song, J.; Kim, S. D.; Kwon, S. H.; Kim, S. K.; Yoon, K. H.; Ahn, B. T. *Thin Solid Films* **1999**, *338*, 13.
(9) Luther, J. M.; Law, M.; Beard, M. C.; Song, Q.; Reese, M. O.; Ellingson, R. J.; Nozik, A. J. *Nano Lett.* **2008**, *8*, 3488.
(10) Zhong, H.; Zhou, Y.; Ye, M.; He, Y.; Ye, J.; He, C.; Yang, C.; Li, Y. *Chem. Mater.* **2008**, *20*, 6434.
(11) Mitzi, D. B.; Yuan, M.; Liu, W.; Kellock, A. J.; Chey, S. J.; Deline, V.; Schrott, A. G. *Adv. Mater.* **2008**, *20*, 3657.
(12) Zhong, H. Z.; Li, Y. C.; Ye, M. F.; Zhu, Z. Z.; Zhou, Y.; Yang, C. H.; Li, Y. F. *Nanotechnology* **2007**, *2*, 18.
(13) Nakamura, H.; Kato, W.; Uehara, M.; Nose, K.; Omata, T.; Otsuka-Yao-Matsuo, S.; Miyazaki, M.; Maeda, H. *Chem. Mater.* **2006**, *18*, 3330.
(14) Castro, S. L.; Bailey, S. G.; Raffaelle, R. P.; Banger, K. K.; Hepp, A. F. *Chem. Mater.* **2003**, *15* (16), 3142.
(15) Kuykendall, T.; Ulrich, P.; Aloni, S.; Yang, P. D. *Nat. Mater.* **2007**, *6*, 951.
(16) Chun, Y. G.; Kim, K. H.; Yoon, K. H. *Thin Solid Films* **2005**, *480*, 46.
(17) Tang, J.; Hinds, S.; Kelley, S. O.; Sargent, E. H. *Chem. Mater.* **2008**, *20*, 6906.
(18) Yang, Y. H.; Chen, Y. T. *J. Phys. Chem. B* **2006**, *110* (35), 17370.
(19) Wei, F.; Zhang, J.; Wang, L.; Zhang, Z. K. *Cryst. Growth Des.* **2006**, *6* (8), 1943.
(20) Horváth, E.; Kukovecz, AÄ k.; Kónya, Z.; Kiricsi, I. *Chem. Mater.* **2007**, *19*, 927.
(21) Zhang, H.; Yang, D.; Li, D.; Ma, X.; Li, S.; Que, D. *Cryst. Growth Des.* **2005**, *5* (2), 547.
(22) Wei, S. H.; Zunger, A. *J. Appl. Phys.* **1995**, *78*, 3846.
(23) Guo, Q.; Ford, G. M.; Hillhouse, H. W.; Agrawal, R. *Nano Lett.* **2009**, *9* (8), 3060.
(24) Stanbery, B. J. *Crit. Rev. Solid State Mater. Sci.* **2002**, *27* (2), 73.
(25) Panthani, M. G.; Akhavan, V.; Goodfellow, B.; Schmidtke, J. P.; Dunn, L.; Dodabalapur, A.; Barbara, P. F.; Korgel, B. A. *J. Am. Chem. Soc.* **2008**, *130*, 16770.
(26) Pan, D.; Wang, X.; Zhou, Z. H.; Chen, W.; Xu, C.; Lu, Y. *Chem. Mater.* **2009**, *21*, 2489.
(27) Llanos, J.; Buljan, A.; Mujica, C.; Ramirez, T. J. *J. Alloys Compd.* **1996**, *234*, 40.
(28) Domashevskayaa, E. P.; Gorbachev, V. V.; Terekhova, V. A.; Kashkarova, V. M.; Panfilova, E. V.; Shchukarev, A. V. *J. Electron Spectrosc. Relat. Phenom.* **2001**, *114−116*, 901.
(29) Goto, T.; Hirai, T. *J. Mater. Sci.* **1988**, *7*, 548.
(30) Calixto, M. E.; Dobson, K. D.; McCandless, B. E.; Birkmire, R. W. *J. Electrochem. Soc.* **2006**, *153*, G521.
(31) Zhou, J.; Bian, G. Q.; Zhang, Y.; Zhu, Q. Y.; Li, C. Y.; Dai, J. *Inorg. Chem.* **2007**, *46* (16), 6347.
(32) Xi, G. C.; Xiong, K.; Zhao, Q. B.; Zhang, R.; Zhang, H. B.; Qian, Y. T. *Cryst. Growth Des.* **2006**, *6*, 577.
(33) Jia, C. H.; Sun, L. D.; Yan, Z. G.; You, L. P.; Luo, F.; Han, X. D.; Pang, Y. C.; Zhang, Z.; Yan, C. H. *Angew. Chem.* **2005**, *117*, 4402.
(34) Contreras, M. A.; Ramanathan, K.; AbuShama, J.; Hasoon, F.; Young, D. L.; Egass, B.; Noufi, R. *Prog. Photovoltaics* **2005**, *13*, 209.